

## Double Transfer Printing of Small Volumes of Liquids

Chaitanya Gupta,<sup>†</sup> Glennys A. Mensing,<sup>‡</sup> Mark A. Shannon,<sup>\*,†,§</sup> and Paul J. A. Kenis<sup>\*,†,‡,§</sup>

Department of Chemical & Biomolecular Engineering, Department of Mechanical Science & Engineering, and Beckman Institute for Advanced Science and Technology, University of Illinois at Urbana-Champaign, Urbana, Illinois 61801

Received November 8, 2006. In Final Form: December 6, 2006

We report here a technique to print small volumes of liquid on a hydrophobic substrate. This process is based on the control of the critical parameters that govern a *quasi-equilibrium* liquid transfer process from one surface to another. We present a qualitative model that describes the physics of a transfer printing process between hydrophobic surfaces, and we use the parameters outlined in this model to manipulate the amount of liquid transferred between surfaces. We demonstrate the printing of discrete, small volumes (~70 fL) of different liquid inks on a polymer substrate starting with volumes that are 8 orders of magnitude larger (a droplet of ~10  $\mu$ L) in a simple two-step procedure.

### Introduction

A variety of transfer printing techniques have been developed over the years, and they have been adapted to multiple applications. Commercial macroscopic printing processes like off-set printing, rotogravure, relief printing, and flexography are a well established, essential component of the publishing, packaging, and transaction printing business.<sup>1</sup> Transfer printing is also used for the commercial production of high density arrays of recognition molecules. In the latter, micromachined quill pens dispense nanoliter volumes of biological “ink” (DNA, proteins, etc.) onto substrates, thereby creating large pixelated arrays of these recognition molecules.<sup>2</sup> The resulting microarrays have emerged as a powerful tool for the quantitative analysis of gene expression,<sup>3,4</sup> protein recognition,<sup>5,6</sup> and identification of potential drug targets.<sup>7,8</sup>

A number of micro- and/or nanoscale printing techniques with striking analogies to macroscopic writing and printing methods have been reported in the literature.<sup>9–21</sup> For example, micro-contact printing uses a stamp fabricated by casting an elastomer

against a master with photolithographically defined relief features on its surface. The stamp and the substrate surfaces are brought into conformal contact to transfer ink from the positive relief features on the stamp to the substrate surface.<sup>9</sup> Micro-contact printing has found many applications including the printing of protein patterns,<sup>10</sup> polymer patterns,<sup>11</sup> microelectrode arrays,<sup>12,13</sup> organic light emitting diodes,<sup>14</sup> and organic thin film transistors.<sup>15</sup> Variations of micro-contact printing have enabled the patterning of sub-100-nm features on a variety of substrates.<sup>16–19</sup> Reactive wet stamping<sup>20</sup> is a similar transfer process that has recently been cited, that utilizes patterned agarose or polyacrylamide stamps to deliver liquid reagents onto substrates in a controllable manner. The transfer of solvated chemicals onto surfaces facilitates in situ reactions that have applications in surface wettability modification, fabrication of large aspect ratio microstructures, and preparation of self-assembly templates.<sup>21,22</sup> Another example of a micro/nanoscale printing technique is dip pen nanolithography (DPN)<sup>23</sup> in which a scanning probe (e.g., an AFM tip) is used to “write” patterns of monolayers of different organic molecules with a resolution down to 5 nm. DPN utilizes a water meniscus, which forms naturally between a tip and sample surface at ambient relative humidity, to serve as the ink transport medium. Diffusion of ink from the probe to the substrate, via the meniscus, is the primary mechanism of transfer in this process.<sup>24</sup>

All these micro/nanoscale printing techniques involve the transfer of liquid from one surface to another. The transfer of liquid droplets of microliter volumes from one solid surface to

\* Corresponding authors: mshannon@uiuc.edu; kenis@uiuc.edu.

<sup>†</sup> Department of Chemical & Biomolecular Engineering.

<sup>‡</sup> Department of Mechanical Science & Engineering.

<sup>§</sup> Beckman Institute for Advanced Science and Technology.

(1) Rotogravure. <http://en.wikipedia.org/wiki/Rotogravure> (June 2006)

(2) Smith, J. T.; Viglianti, B. L.; Reichert, W. M. *Langmuir* **2002**, *18*, 6289–6293.

(3) DeRisi, J.; Penland, L.; Brown, P. O.; Bittner, M. L.; Meltzer, P. S.; Ray, M.; Chen, Y. D.; Su, Y. A.; Trent, J. M. *Nat. Genet.* **1996**, *14*, 457–460.

(4) Schena, M.; Shalon, D.; Davis, R. W.; Brown, P. O. *Science* **1995**, *270*, 467–470.

(5) Haab, B. B.; Dunham, M. J.; Brown, P. O. *Genome Biology* **2001**, *2*, RESEARCH0004.

(6) MacBeath, G.; Schreiber, S. L. *Science* **2000**, *289*, 1760–1763.

(7) Brody, E. N.; Willis, M. C.; Smith, J. D.; Jayasena, S.; Zichi, D.; Gold, L. *Mol. Diagn.* **1999**, *4*, 381–8.

(8) Yowe, D.; Cook, W. J.; Gutierrez-Ramos, J. C. *Microbes Infect.* **2001**, *3*, 183–21.

(9) Xia, Y. N.; Whitesides, G. M. *Angew. Chem., Int. Ed.* **1998**, *37*, 551–575.

(10) Bernard, A.; Delamar, E.; Schmid, H.; Michel, B.; Bosshard, H. R.; Biebuyck, H. *Langmuir* **1998**, *14*, 2225–2229.

(11) Jeon, N. L.; Choi, I. S.; Whitesides, G. M.; Kim, N. Y.; Laibinis, P. E.; Harada, Y.; Finnie, K. R.; Girolami, G. S.; Nuzzo, R. G. *Appl. Phys. Lett.* **1999**, *75*, 4201–4203.

(12) He, H. X.; Li, Q. G.; Zhou, Z. Y.; Zhang, H.; Li, S. F. Y.; Liu, Z. F. *Langmuir* **2000**, *16*, 9683–9686.

(13) Breen, T. L.; Fryer, P. M.; Nunes, R. W.; Rothwell, M. E. *Langmuir* **2002**, *18*, 194–197.

(14) Koide, Y.; Wang, Q. W.; Cui, J.; Benson, D. D.; Marks, T. J. *J. Am. Chem. Soc.* **2000**, *122*, 11266–11267.

(15) Kagan, C. R.; Breen, T. L.; Kosbar, L. L. *Appl. Phys. Lett.* **2001**, *79*, 3536–3538.

(16) Kumar, A.; Biebuyck, H. A.; Abbott, N. L.; Whitesides, G. M. *J. Am. Chem. Soc.* **1992**, *114*, 9188–9189.

(17) Wang, D. W.; Thomas, S. G.; Wang, K. L.; Xia, Y. N.; Whitesides, G. M. *Appl. Phys. Lett.* **1997**, *70*, 1593–1595.

(18) Jackman, R. J.; Wilbur, J. L.; Whitesides, G. M. *Science* **1995**, *269*, 664–666.

(19) Xia, Y. N.; Rogers, J. A.; Paul, K. E.; Whitesides, G. M. *Chem. Rev.* **1999**, *99*, 1823–1848.

(20) Fialkowski, M.; Campbell, C. J.; Bensemann, I. T.; Grzybowski, B. A. *Langmuir* **2004**, *20*, 3513.

(21) Campbell, C. J.; Smoukov, S. K.; Bishop, K. J. M.; Grzybowski, B. A. *Langmuir* **2005**, *21*, 2637–2640.

(22) Klajn, R.; Fialkowski, M.; Bensemann, I. T.; Bitner, A.; Campbell, C. J.; Bishop, K. J. M.; Smoukov, S. K.; Grzybowski, B. A. *Nat. Mater.* **2004**, *3*, 729–735.

(23) Hong, S. H.; Zhu, J.; Mirkin, C. A. *Science* **1999**, *286*, 523–525.

(24) Piner, R. D.; Mirkin, C. A. *Langmuir* **1997**, *13*, 6864.

another was first investigated by Chadov and Yakhnin.<sup>25,26</sup> They studied the transfer process under quasi-equilibrium conditions and as a function of the rate of retraction of the stamp from the substrate, for liquids with different values of surface tension and viscosity. Their observations were key to identifying the parameters that influence pattern fidelity in microscale off-set printing.<sup>27,28</sup> These studies investigated the transfer of liquids from hydrophilic stamp surfaces to hydrophilic or hydrophobic substrates. Furthermore, a number of efforts to describe the shape<sup>29–36</sup> and stability<sup>37–39</sup> of liquid bridges between solid surfaces have been reported in literature.

In this paper, we identify the critical parameters that determine the amount of liquid transferred from one *hydrophobic* surface to another *hydrophobic* surface in a quasi-equilibrium liquid transfer process, and we propose a qualitative model that describes the physics underlying this process. We also demonstrate the controlled transfer of small volumes of liquid, down to the femtoliter regime, from an initial drop that is several microliters in volume, using a straightforward two-step transfer procedure.

### Experimental Details

**Surface Preparation.** Gold-coated samples were obtained by sputtering 60 nm chrome followed by 100 nm gold on a diced 2 × 1 cm<sup>2</sup> silicon wafer fragment (<100>, n doped, resistivity 8–20 Ω cm, Silicon Quest International, Santa Clara, CA). They were washed in SC-1 solution (100 mL of deionized (DI) water/10 mL of H<sub>2</sub>O<sub>2</sub>/1 mL of NH<sub>4</sub>OH), sonicated in acetone/IPA and blow dried with N<sub>2</sub> prior to use. The DI water (resistivity 18 MΩ cm) source was an in-house line. PDMS (Sylgard 184, Dow Corning, Midland, MI) was prepared as a 1:10 mixture of cross-linker/polymer ratio, which was degassed, spin-coated onto a 4 in. silicon wafer, and cured at 70 °C for 5 h. Rectangles (2 × 1 cm<sup>2</sup> in dimensions) were cut out of the molded PDMS film. Sheets of two types of biomedical grade, nonreinforced vulcanized silicone (880151/NV10 and 880151/NV20, Medisil Corp., Ventura, CA) were also cut into 2 × 1 cm<sup>2</sup> rectangles. The two silicone-based surfaces will be subsequently referred to as silicone A and silicone B, respectively. Prior to use, all polymer surfaces were cleaned by sonication in acetone/IPA for 15 min, followed by drying in a vacuum oven at 40 °C for 3 h. Elastomeric stamps with positive relief features (posts, pyramids) were prepared by casting PDMS against a master with complementary features etched onto its surface. The master for postrelief features was created by dry etching (BOSCH process, PlasmaTherm 2000 ICP-DRIE etching system) cylindrical holes of varying diameters into a silicon wafer. Positive photoresist AZ4620 (Hoechst Celanese Corp., Somerville, NJ) served as the etch mask for the dry etch process. Pyramid-shaped holes were wet etched (35% KOH, 59% DI, 6% IPA at 85 °C) into a <100> n-doped silicon wafer surface. Square holes of varying side lengths were photolithographically patterned

in positive photoresist, and the pattern was transferred onto a silicon nitride film (ASM LPCVD system) of 500 nm thickness by dry etching (SF<sub>6</sub>, Ar isotropic etch, PlasmaTherm2000 ICP-DRIE system). The patterned SiN<sub>x</sub> film was subsequently used as the mask for the wet etch. The size of the square holes determined the width of the tip of the pyramid shaped relief structure.

**Droplet Visualization.** To visualize the smallest printed droplets, we used different inks: fluorescent nanoparticles (20 nm Fluorospheres, Invitrogen Corp., Carlsbad, CA), AF488 hydroxylamine dye (A30629, Invitrogen), AF647 hydroxylamine dye (A30632, Invitrogen), 5 nm colloidal gold conjugate and AF488 labeled streptavidin (A32360, Invitrogen), tetramethylrhodamine biocytin (T12921, Invitrogen), and amino-PEG quantum dots (Q21541MP, Invitrogen). All inks were diluted to a 1:100 mixture using a stock solution of 90% phosphate buffer (mixture of potassium mono- and dihydrogen phosphate in DI, buffered at pH 7), 10% glycerol (Sigma-Aldrich, St. Louis, MO), and 1 mM fructose sugar (Sigma-Aldrich).

**Surface Characterization.** For all surfaces used in this study, the advancing ( $\theta_A$ ), receding ( $\theta_R$ ), and static ( $\theta_S$ ) contact angles were measured using a goniometer (CAM 100, KSV, Finland). The advancing angle is defined as the largest contact angle observed before the three-phase line between the surface, the liquid, and air advances on the substrate, while the receding angle is the smallest observed angle during the recession of the contact line.<sup>40</sup> Results for the surfaces used are as follows: PDMS,  $\theta_A = 118^\circ \pm 3^\circ$ ,  $\theta_R = 85^\circ \pm 3^\circ$ ,  $\theta_S = 105^\circ \pm 1^\circ$ ; gold,  $\theta_A = 62^\circ \pm 3^\circ$ ,  $\theta_R = 10^\circ \pm 3^\circ$ ,  $\theta_S = 32^\circ \pm 1^\circ$ ; silicone A,  $\theta_A = 120^\circ \pm 3^\circ$ ,  $\theta_R = 65^\circ \pm 3^\circ$ ,  $\theta_S = 115^\circ \pm 1^\circ$ ; and silicone B,  $\theta_A = 110^\circ \pm 3^\circ$ ,  $\theta_R = 60^\circ \pm 3^\circ$ ,  $\theta_S = 95^\circ \pm 1^\circ$ .

**Printing Experiments.** A fixed volume of liquid is applied onto a surface using a pipet (XL3000i, Denville Scientific, Metuchen, NJ), and this surface, which we will refer to as the “substrate” in this study, is mounted on a XY stage (KSV, Finland). The second surface, which we will refer to as the “gripper”, is mounted on a Z stage (KSV) parallel to the substrate. The micrometer on the Z stage is used to control the distance  $h$  between the gripper and the substrate. Figure 1 illustrates the configuration of the setup and a typical liquid transfer sequence. Each transfer experiment is visualized with a high-speed camera (DMK 21F04, Imaging Source Inc., Charlotte, NC) at 30 frames/s. Each experimental run was repeated thrice. The experiments are conducted in a class 100 clean-room environment at a relative humidity of 34%. Drop shape analysis software (KSV) is used to calculate droplet volumes. The volume of liquid transferred is determined by measuring the difference between the volumes of the droplet on the substrate before and after the transfer process. Droplets with diameters less than 20 μm were visualized by mounting the substrate on cover-glass (S175212, Fisher Scientific, Pittsburgh, PA), and the surface of the substrate, on which the droplet was transferred via the gripper mounted on a Z stage, was imaged through the cover-glass using an inverted microscope (Leica DMIRE2, Leica Microsystems, Bannockburn, IL) at 50× magnification. Images were captured with a CCD camera (Retiga Exi FAST, Qimaging Corp., Burnaby, Canada), at 2 frames/s using Image-Pro Plus software (Media Cybernetics, Silver Spring, MD).

### Results and Discussion

In this paper, we first identify the parameters that influence the amount of liquid transferred from one hydrophobic surface (the substrate) to another hydrophobic surface (the gripper) beginning with the situation where the droplet forms a liquid bridge between those two surfaces, and we introduce a model that can qualitatively explain our observations. On the basis of our understanding of the liquid transfer process, we then describe a two-step transfer printing procedure which enables the printing of femtoliter volumes of liquids from starting volumes that are 8 orders of magnitude larger. The liquid on the substrate is brought into contact with the gripper, which subsequently is retracted at

(25) Chadov, A. V.; Yakhnin, E. D. *Colloid J. Russian Academy of Sciences* **1979**, *41*, 817.

(26) Yakhnin, E. D.; Chadov, A. V. *Colloid J. Russ. Acad. Sci.* **1983**, *45*, 1183.

(27) Darhuber, A. A.; Troian, S. M.; Wagner, S. J. *Appl. Phys.* **2001**, *90*, 3602.

(28) Darhuber, A. A.; Miller, S. M.; Troian, S. M.; Wagner, S. J. *Appl. Phys.* **2000**, *88*, 5119.

(29) Melrose, J. C. *AIChE J.* **1966**, *12*, 986.

(30) Boucher, E. A.; E., M. J. B. *Proc. R. Soc. London, Ser. A* **1975**, *346*, 349–374.

(31) Boucher, E. A.; Evans, M. J. B.; Kent, H. J. *Proc. R. Soc. London, Ser. A* **1976**, *349*, 81–100.

(32) Boucher, E. A.; Kent, H. J. *Proc. R. Soc. London, Ser. A* **1977**, *356*, 61–75.

(33) Boucher, E. A. *Rep. Prog. Phys.* **1980**, *43*, 497–546.

(34) Boucher, E. A.; E., M. J. B. *J. Colloid Interface Sci.* **1980**, *75*, 409–418.

(35) Boucher, E. A.; Evans, M. J. B.; McGarry, S. J. *Colloid Interface Sci.* **1982**, *89*, 154–165.

(36) Boucher, E. A.; Jones, T. G. J. *J. Colloid Interface Sci.* **1988**, *126*, 469–481.

(37) Gillette, R. D.; Dyson, D. C. *J. Chem. Eng.* **1971**, *2*, 44–54.

(38) Cryer, S. A.; Steen, P. A. *J. Colloid Interface Sci.* **1992**, *154*, 276–288.

(39) Peppin, X.; Rossetti, D.; Iveson, S. M.; Simons, S. J. R. *J. Colloid Interface Sci.* **2000**, *232*, 289–297.

(40) Neumann, A. W. *Adv. Colloid Interface Sci.* **1974**, *4*, 105–191.

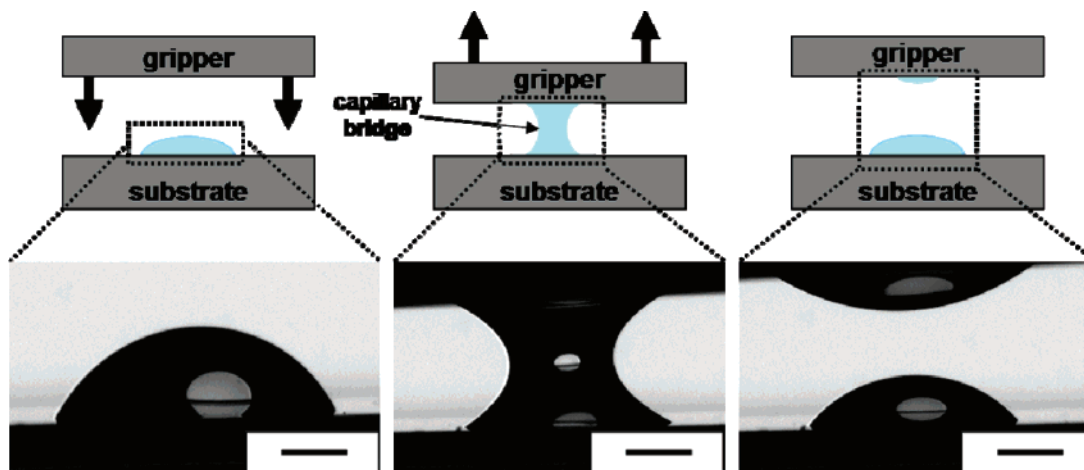


**Figure 1.** Schematic of the steps in the transfer printing process of an amount of liquid from one surface to another surface: First, a gripper surface is lowered (left) and brought into contact with the liquid droplet on the substrate (middle). Then, the gripper is retracted at a finite velocity until the capillary bridge between the gripper and the substrate breaks (right). Scale bar: 750  $\mu\text{m}$ .

a constant velocity from the substrate, resulting in transfer of a fraction of the liquid to the gripper surface (Figure 1). The largest volume of liquid used in these experiments is a droplet of 5  $\mu\text{L}$  with a radius of 1 mm, which is less than the capillary length for water ( $\sim 3$  mm).<sup>41</sup> Thus, gravity does not play a significant role in these experiments, which was confirmed experimentally as well. The retraction velocities ( $V$ ) employed are such that the maximum values of the Reynolds number ( $Re$ ) and the capillary number ( $Ca$ ) for these experiments are 0.05 and 0.003, respectively.

**Identification of Critical Parameters.** Figure 2a compares the extent of transfer for two different gripper materials: silicone A ( $\theta_S = 115^\circ \pm 1^\circ$ ,  $\theta_R = 65^\circ \pm 3^\circ$ ) and silicone B ( $\theta_S = 95^\circ \pm 1^\circ$ ,  $\theta_R = 60^\circ \pm 3^\circ$ ). The substrate used for both transfer experiments was PDMS ( $\theta_S = 105^\circ \pm 1^\circ$ ,  $\theta_R = 85^\circ \pm 3^\circ$ ). For a given liquid (water), a fixed volume (1.4  $\mu\text{L}$ ), zero initial compression of the liquid bridge between the two surfaces, and fixed gripper velocity (25  $\mu\text{m/s}$ ), complete transfer of the droplet from the PDMS substrate to either gripper material is observed (Figure 2a). In subsequent experiments, we investigated the effect of other factors that determine the amount of liquid transferred like total droplet volume, liquid viscosity and surface tension, initial extent of compression, and retraction velocity of the gripper.

For all experiments shown in Figures 2b–f, the substrate is PDMS and the gripper is silicone A. Figure 2b indicates that a decrease in volume of the droplet from 5  $\mu\text{L}$  (1–3) to 1.7  $\mu\text{L}$  (4–6) increases the percentage of liquid transferred from the PDMS substrate to the silicone gripper. Figure 2c depicts the difference in transfer for two different initial conditions. For experiments 1–3 in Figure 2c, the gripper is lowered until it just contacts the droplet, and then it is retracted at a velocity of 50  $\mu\text{m/s}$ . In experiments 4–6, the droplet volume is compressed to half of the height started from in experiments 1–3 such that the radius of the contact circles at the two surfaces is about 1.5 times larger than that for experiments 1–3. Before the start of the actual liquid transfer experiment by retraction of the gripper, the liquid droplet was compressed at a velocity of  $\sim 1$  mm/s. Upon retraction of the gripper at the same velocity of 50  $\mu\text{m/s}$ , it becomes apparent that a large initial compression results in nearly complete transfer of the droplet from the PDMS surface (substrate) to the silicone surface (gripper).

Figure 2d depicts the difference in the amount of liquid transferred for two different gripper retraction rates, 50 and 25

$\mu\text{m/s}$  for experiments 1–3 and 4–6, respectively. A larger volume of liquid is transferred in the experiments with a slower gripper retraction velocity. Experiments 4–6 in Figure 2c, however, indicate that as long as the liquid bridge was compressed initially, complete transfer is possible at higher gripper retraction velocities.

Next we investigated the influence of fluid properties on the amount of liquid transferred. The viscosity and surface tension values for water are  $10^{-3}$  kg/(m s) and 0.073 N/m, respectively. Complete transfer of a water droplet from the PDMS surface to the silicone gripper is observed at a gripper retraction velocity of 25  $\mu\text{m/s}$  (experiments 1–3, Figure 2e). Glycerol, on the other hand, has a surface tension of 0.064 N/m that is comparable to water, but its viscosity is 3 orders of magnitude higher at 1.49 kg/(m s). An incomplete transfer of glycerol is observed at the same gripper retraction velocity (experiments 4–6, Figure 2e), which indicates the importance of the relative magnitudes of the surface tension to viscous forces of the liquid to be transferred during the printing processes.

Figure 2f shows the effect of initial compression of the droplet on the extent of transfer for water and glycerol droplets. In contrast to the experiment shown in Figure 2e, in which glycerol transferred only partially, both a water droplet (experiments 1–3, Figure 2f) and a glycerol droplet (experiments 4–6, Figure 2f) are transferred almost completely from the PDMS substrate to the silicone A gripper when the droplet is compressed initially. Although compressing the droplet, as before at 1 mm/s, makes the contact line advance on the substrate and the gripper surfaces, we did not observe any correlation of transfer with the advancing contact angle,  $\theta_A$ , in keeping with the observations made by Chadov and Yakhnin.<sup>25,26</sup>

Figure 3 compares the transfer characteristics for three PDMS surfaces with different positive relief features. In these experiments, gold is the substrate and the gripper is the PDMS surface with the structural features. The experiment begins with an uncompressed, 5  $\mu\text{L}$  droplet of water on the substrate. In Figure 3a, the molded feature on the PDMS surface is a shallow (depth  $\sim 8$   $\mu\text{m}$ ) hole of 200  $\mu\text{m}$  diameter. In this experiment, the substrate is lowered until the water droplet touches the PDMS surface. Once the meniscus forms, the substrate is retracted away from the gripper at a velocity of 25  $\mu\text{m/s}$ . A droplet with a diameter equal to that of the hole is transferred to the PDMS surface and it is confined within the hole. The features on the PDMS surfaces in experiments b and c of Figure 3 are a single post and a truncated pyramid, respectively. The diameter of the post and the width

(41) Decker, E. L.; Garoff, S. *Langmuir*. **1997**, *13*, 6321–6332.

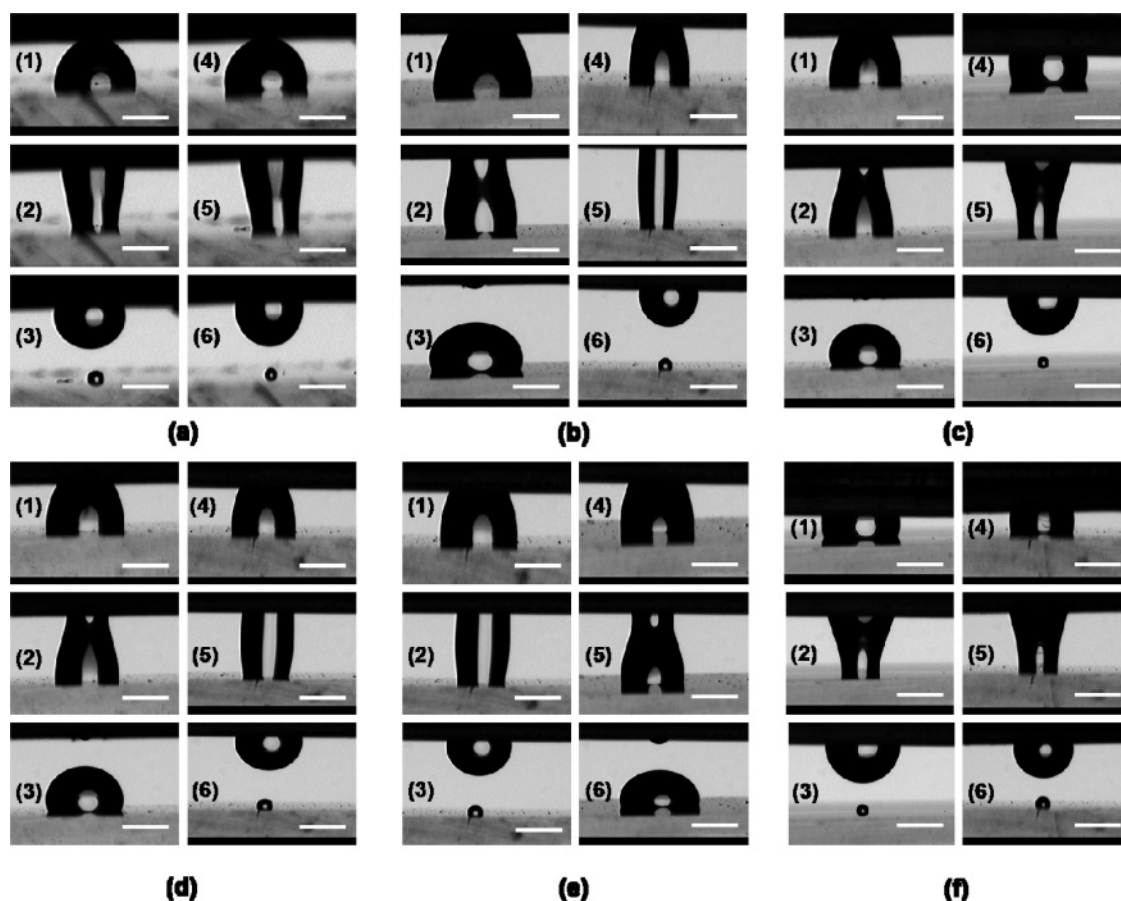


**Figure 2.** Optical micrographs of the transfer of liquid from a substrate (PDMS, bottom) to a gripper (silicone A, top; unless otherwise noted). For all experiments, unless otherwise noted, the retraction velocity of the gripper is  $25 \mu\text{m/s}$ , and the droplet was initially not compressed. Scale bars: 1 mm. Each set of images (1)–(3) and (4)–(6) corresponds to the steps shown schematically in Figure 1. (a) (1)–(3) Transfer of water to a relatively hydrophilic gripper (silicone B). (4)–(6) Transfer of water to a relatively hydrophobic gripper (silicone A). Volume of droplet =  $1.4 \mu\text{L}$ . (b) (1)–(3) Transfer of a large droplet of water ( $5 \mu\text{L}$ ). (4)–(6) Transfer of a small droplet of water ( $1.7 \mu\text{L}$ ). (c) (1)–(3) Transfer of water for small initial compression. (4)–(6) Transfer of water for large initial compression. Gripper retraction velocity =  $50 \mu\text{m/s}$ . Volume of droplet =  $1.7 \mu\text{L}$ . (d) (1)–(3) Transfer of water for large gripper retraction velocity ( $50 \mu\text{m/s}$ ). (4)–(6) Transfer from PDMS for small gripper retraction velocity ( $25 \mu\text{m/s}$ ). Volume of droplet =  $1.8 \mu\text{L}$ . (e) (1)–(3) Transfer of water. (4)–(6) Transfer of glycerol. Volume of droplet =  $1.8 \mu\text{L}$ . (f) (1)–(3) Transfer of water. (4)–(6) Transfer of glycerol. Volume of droplet =  $1.6 \mu\text{L}$ . Large initial compression.

of the tip of the truncated pyramid are each  $200 \mu\text{m}$ . In these experiments, the gripper is retracted away from the substrate at a velocity of  $25 \mu\text{m/s}$ . The amount of liquid transferred to the post structure (Figure 3b) is less than the volume of liquid transferred to the pyramid feature (Figure 3c), which, in turn, is less than the volume of liquid transferred to the shallow hole feature (Figure 3a). The tip of the post and the pyramid relief structures will be referred to as the “print-head” in all subsequent experiments.

Figure 4 compares the amounts of liquid transferred to the post (parts a and b of Figure 4) and truncated pyramid (parts c and d of Figure 4) from different substrates (gold, silicone A and PDMS). At the start of the experiment, an uncompressed water droplet is placed between the substrate and the gripper, and the gripper is retracted at a velocity of  $25 \mu\text{m/s}$ . The largest amounts of liquid are transferred from the PDMS substrates, and the gold substrates transfer the minimum amount of liquid to the gripper in each case (post and pyramid). The amount of liquid transferred decreases with a reduction in the print-head size. A comparison of the volumes of liquid transferred to a pyramidal feature and a post relief structure at the same print-head size reveals that a greater volume of liquid is transferred to the pyramidal print-head. A smaller initial volume ( $0.4 \mu\text{L}$ ) of liquid on the substrate (parts b and d of Figure 4) results in a greater percentage of liquid

being transferred to either kind of gripper compared to the case that started with a larger initial volume ( $4 \mu\text{L}$ ) of liquid on the substrate (parts a and c of Figure 4), which is in full agreement with our earlier observations shown above (Figure 2b).

**Mechanism of Liquid Transfer between Surfaces.** On the basis of the experimental observations in Figure 2, we hypothesize the following two-step mechanism of transfer: Step 1 describes the initiation of motion at the three-phase line. The surface tension at the liquid–vapor interface of the liquid bridge pulls on the liquid molecules at the three-phase contact line on each of the two surfaces. The molecules of liquid at each of the three-phase contact lines also experience forces of attraction from their respective solid phases (Figure 5a). A molecule at the contact line that is attempting to diffuse along the liquid–vapor interface and away from the solid surface would have to overcome the forces of attraction due to the solid phase. Thus, the position that any molecule at the contact line occupies on the solid surface in the static case may be thought of as a free energy well, surrounded by energy barriers corresponding to the onset of diffusive migration by these molecules (Figure 5b). The location of the free energy minimum that represents the static liquid meniscus ( $\theta_s$ ) is a function of the strength of the forces of attraction between the liquid and solid phase. For a polar liquid molecule on a hydrophilic surface ( $\theta_s < 90^\circ$ ), the molecule has a lower

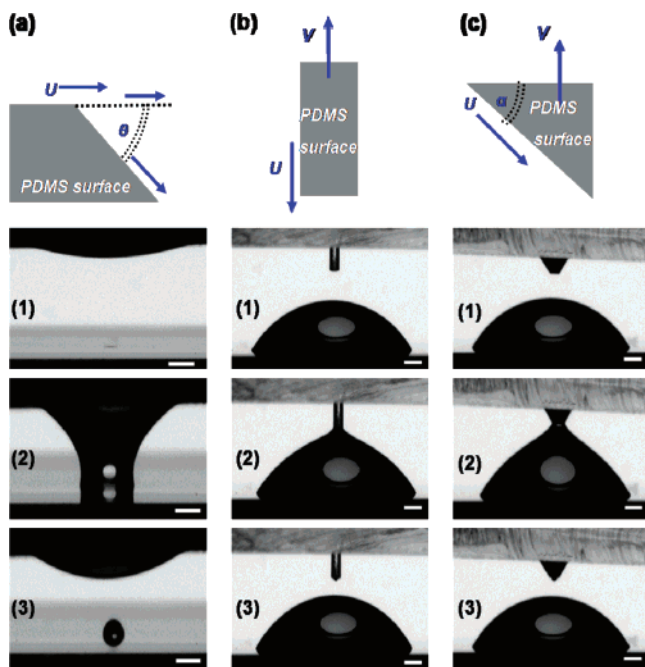


**Figure 3.** Optical micrographs of transfer of liquid to a PDMS gripper. For all experiments, unless otherwise noted, the retraction velocity of the gripper is  $25 \mu\text{m/s}$ , the liquid used is water, and the initial volume of liquid is  $5 \mu\text{L}$ . The substrate used is gold in each case. Each image in (1)–(3) corresponds to the steps shown schematically in Figure 1. The three schemes at the top represent the direction of contact line motion relative to the gripper surface. All scale bars are  $400 \mu\text{m}$ . (a) Transfer of water to a PDMS stamp patterned with a shallow holelike relief. Hole size is  $200 \mu\text{m}$ . (b) Transfer of water to a PDMS stamp patterned with a pillar relief structure. Diameter of pillar tip is  $200 \mu\text{m}$ . (c) Transfer of water to a PDMS stamp patterned with a pyramid relief structure. Width of pyramid tip is  $200 \mu\text{m}$ .

free energy than if it were forming a static meniscus on a hydrophobic surface ( $\theta_S > 90^\circ$ ). However, the difference in the free energies corresponding to  $\theta_S$  is not as significant for the case where the polar liquid molecule is in contact with two different hydrophobic surfaces, i.e., the difference in the free energy for the static liquid meniscus is not as significant for liquid transfer between PDMS and silicone A and between PDMS and silicone B as it is for liquid transfer between PDMS and gold.

The description of static and dynamic contact angles in terms of an activation energy for diffusive migration was first described by Cherry et al.<sup>42</sup> and subsequently expanded on by Hoffman.<sup>43</sup> Transfer of a polar liquid between surfaces with a large difference in static contact angle ( $\theta_S$ ) would be from the surface with the higher static contact angle (like silicone A) to the surface with lower static contact angle (like gold). Less work is required to dislodge the molecules of liquid at the three-phase line on the hydrophobic surface. Surface characterization in terms of the static contact angle alone, however, is insufficient to explain why water transfers completely from PDMS to silicone A and from PDMS to silicone B, even though it may suffice as an explanation for why water transfers completely from silicone A to gold. Evidently, a parameter other than the static contact angle describes the work done to initiate movement of the three-phase line when a polar liquid is being transferred between two hydrophobic surfaces ( $\theta_S > 90^\circ$ ). As the separation between the two surfaces increases, the pull exerted by the surface tension

on the molecules at the three-phase line increases. The magnitude of this surface tension force is a function of the evolving shape of the liquid bridge between the two solid surfaces. The liquid–vapor interface distorts from its equilibrium shape and the contact angle decreases from its static value ( $\theta_S$ ) at both surfaces to its receding value ( $\theta_R$ ). The increasing capillary force along the liquid–vapor interface decreases the potential energy barrier by a  $\Delta G_{\text{diff}}$  (Figure 5b), thus making it easier for the molecule to move away from the solid surface.<sup>43</sup> Thus, the difference between the receding and static contact angles is a measure of the magnitude of distortion in the activation energy curve that is required to initiate actual motion of the contact line, which is the onset of step 2 of the proposed mechanism. The three-phase contact line thus begins to move first on the surface with the least difference between the static and receding contact angles, which, in our experiments, is PDMS. This model explains why water is transferred completely from PDMS to silicone A and silicone B (Figure 2a, experiments 1–3 and 4–6).

Step 2 of the liquid transfer process involves the steady-state kinematics of the three-phase contact line at the two solid surfaces (Figure 5c,d). At steady state, when the contact line moves in the  $-x$  direction, at speed  $U$  with respect to a ground frame of reference, the molecules of liquid at the solid surface have a velocity component of  $U$  in the  $x$  direction with respect to a set of reference axes that have their origin at the location of the contact line (Figure 5c). The molecules of liquid at the contact line have a velocity component  $U \sin \phi$  in the  $z$  direction, which determines the speed with which liquid is removed from the solid surface (Figure 5d), where  $\phi$  is the angle between the liquid–vapor interface and solid surface. This rolling motion within the frame of reference attached to the contact line shows that the motion of the contact line does not violate the no-slip boundary condition as elaborated on by Dussan et al.<sup>44</sup> The steady-state velocity of the contact line  $U$  depends on the relative importance of the viscous forces to the surface tension forces, where for two liquids with comparable surface tension values but differing viscosities the three-phase contact line would move at a faster rate for the less viscous liquid. Once the contact line is moving, the velocity of the retracting gripper must be matched to the vertical velocity component  $U \sin \phi$  of molecules at the moving contact line on the substrate. If the gripper retraction velocity is higher than the rate at which liquid molecules are removed from the substrate (i.e., the liquid cannot keep pace), the liquid transfers only partially from the substrate before the liquid bridge breaks. When the two velocities are comparable, or the gripper retraction rate is much slower than  $U \sin \phi$ , almost complete transfer of the droplet from the substrate is observed before the liquid bridge breaks (Figure 2d, experiments 1–3 and 4–6).

Chadov and Yakhnin also reached a similar conclusion about the pivotal role of the receding angle in liquid transfer between surfaces.<sup>25</sup> However, their arguments for the receding angle were based solely on geometric considerations, and they determined that  $\theta_R$  was the only parameter that determined the direction of liquid transfer in the quasi-static case. In a subsequent paper they argued that the effects of gripper retraction velocity, liquid surface tension, and viscosity played an important role only in the nonequilibrium cases.<sup>26</sup> Our observations in Figure 2 lie in a regime where  $Re, Ca \ll 1$ . A small Reynolds number ( $Re$ ) guarantees quasi-static flow conditions because the time scale associated with the gripper retraction is much larger than the time scale for the diffusion of momentum, and a low value of the capillary number ( $Ca$ ) puts our observations in the regime where surface tension effects dominate over viscous dissipation.

(42) Cherry, B. W.; Holmes, C. M. *J. Colloid Interface Sci.* **1969**, *29*, 174–176.

(43) Hoffman, R. L. *J. Colloid Interface Sci.* **1983**, *94*, 470–486.

(44) Dussan, E. B. V. *Annu. Rev. Fluid Mech.* **1979**, *11*, 371–400.

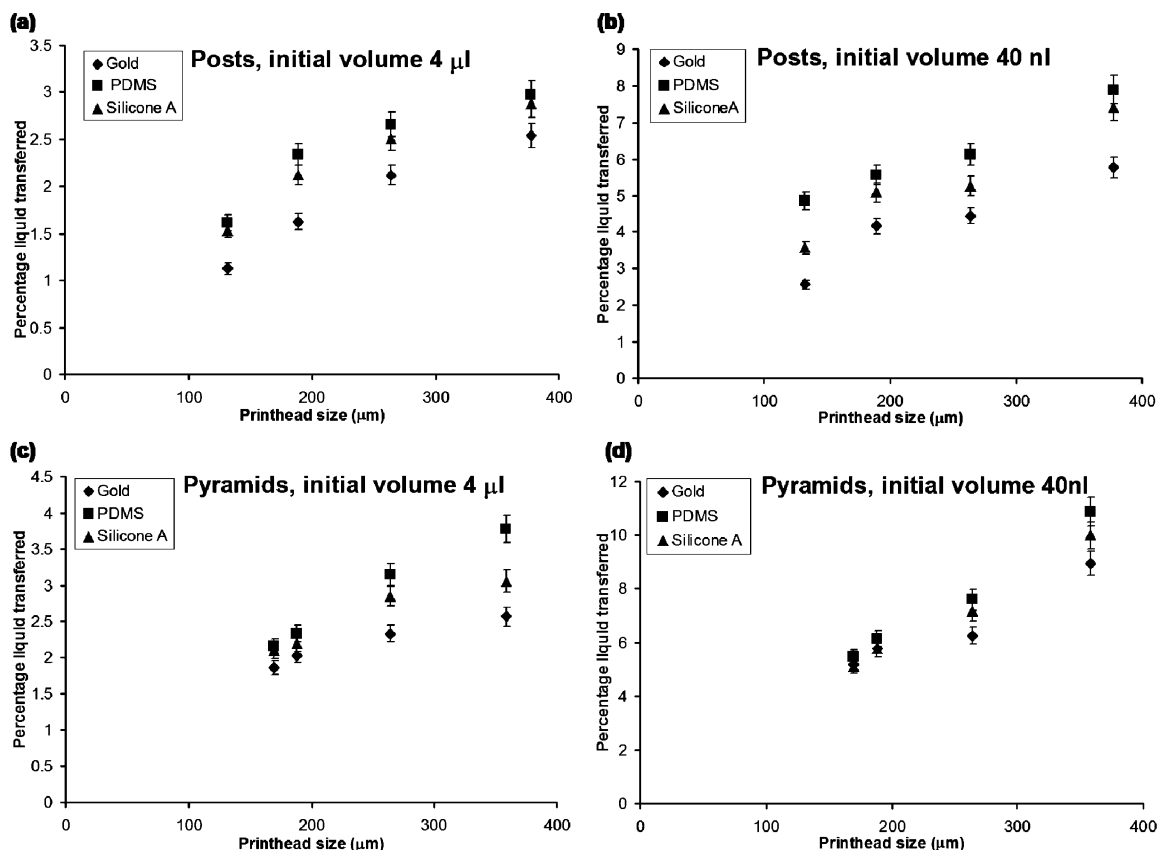


**Figure 4.** Percentage liquid transferred versus print-head size for post-shaped relief features on PDMS gripper, using an initial droplet volume of (a)  $4 \mu\text{L}$  and (b)  $40 \text{ nL}$ . Percentage liquid transferred versus print-head size for pyramid-shaped relief features on PDMS gripper, using an initial droplet volume of (c)  $4 \mu\text{L}$  and (d)  $40 \text{ nL}$ . For all experiments, unless otherwise noted, the gripper retraction velocity is  $25 \mu\text{m/s}$ , the liquid used is water, and the substrates used are gold, silicone A, and PDMS.

Despite the fact these experiments are in the quasi-static, surface energy dominated regime, our observations for *hydrophobic* surfaces seem to indicate the importance of parameters like gripper retraction velocity, liquid volume, surface tension, and viscosity of the liquid and the initial compression of the droplet on the final outcome of the transfer process. A possible explanation for the apparent anomaly might lie in the fact that experimental observations by Chadov and Yakhnin were concerned with transfer from hydrophilic substrates only. As we pointed out in the discussion above, all hydrophilic surfaces would have a large potential energy barrier to the onset of migration of liquid molecules away from the solid surface. Thus, the transfer of liquid from hydrophilic substrates would be characterized by little or no motion of the three-phase contact line during the period when the meniscus is intact. Therefore, the parameters that affect contact line motion for *hydrophobic* surfaces might not have any effect on the transfer process for *hydrophilic* surfaces.

Compression of the liquid droplet results in a larger initial contact area on both surfaces, thus resulting in greater adhesion of the capillary bridge at each of the two surfaces. Although compression results in an advancing contact line on both surfaces, the large compression velocity ( $\sim 1 \text{ mm/s}$ ) imposed on the gripper surface controls the rate of spreading and thus the initial conditions of the geometry of the liquid upon retraction. The advancing contact angle ( $\theta_A$ ) itself is at most a second-order effect in the transfer of liquids, matching the observation that the advancing angle does not correlate to the extent of transfer. The initial size of the droplet and the retraction rate, however, do correlate strongly to the transfer. Retraction of the gripper initiates movement of the three-phase contact line on the surface with the lower difference between receding and static contact angle. The

larger adhesion force at one surface creates a larger pull on the three-phase contact line of the other surface with the lower receding-static contact angle difference. As a result, the contact line on the surface with the lower receding-static contact angle difference begins to move sooner and with greater velocity, if the droplet is compressed initially as compared to the case without the initial compression of the droplet. Thus, with compression, complete transfer is observed at larger gripper velocities (Figure 2c, experiments 4–6). The effect of large initial compression, and subsequently greater three-phase contact line velocities, was also observed for more viscous liquids like glycerol. At a gripper retraction rate of  $25 \mu\text{m/s}$ , complete transfer is seen for the case where the droplet is initially compressed (Figure 2f, experiments 4–6), compared to only partial transfer when the liquid droplet initially is not compressed (Figure 2e, experiments 4–6). Our hypothesized two-step model seems to explain the outcomes of all our experiments, as well as those cited in the literature, without the inclusion of molecular scale forces such as van der Waals, electrostatic, and hydrophobic/hydrophilic structural forces. However, the inclusion of significant amounts of solutes and/or particles in the solution, such as proteins and DNA, may change this result, due to the interaction of the solutes with the solution and surfaces. These interactions may change the  $\Delta G_{\text{diff}}$  and  $U \sin \phi$  associated with the transfer process. Surface roughness affects the transfer process in a similar way. Physical features on solid surfaces are known to trap the three-phase contact line locally,<sup>45,46</sup> which would increase the  $\Delta G_{\text{diff}}$  required to initiate

(45) de Gennes, P. G. *Rev. Mod. Phys.* **1985**, *57*, 827–862.

(46) Joanny, J. F.; de Gennes, P. G. *J. Chem. Phys.* **1984**, *81*, 552–562.

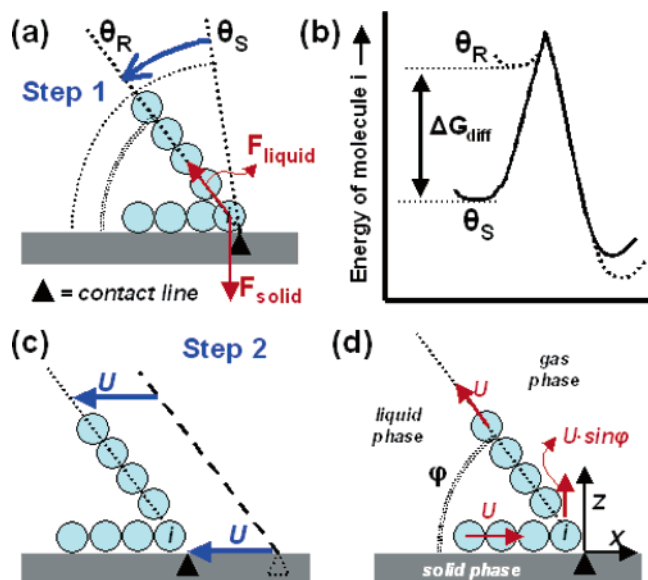


**Figure 5.** Schematic illustrating the proposed two-step transfer mechanism at the three-phase contact line. The blue circles represent the liquid molecules at the contact line between the liquid phase, gas phase, and a solid surface (gray). The contact line position is indicated by the black triangle. (a) Step 1, the pull caused by the retraction of the gripper results in deformation of liquid–vapor meniscus of the liquid bridge, which leads to a change from the static ( $\theta_s$ ) to the receding ( $\theta_R$ ) contact angle. (b) Deformation of the liquid–vapor meniscus as shown in (a) reduces the energy barrier for diffusion of molecule  $i$  from the solid surface to the liquid–vapor interface by  $\Delta G_{\text{diff}}$ . (c) Step 2 with respect to a ground frame of reference; steady-state motion of the contact line in the  $-x$  direction. (d) Step 2 with respect to a frame of reference attached to the contact line position; the solid–liquid and liquid–vapor interfaces roll at velocity  $U$  with respect to the axes frame attached to the contact line position. Velocity of liquid molecules at the solid surface with respect to a ground frame of reference, as shown in (c), is zero, thereby obeying the no-slip boundary condition.

motion and effectively decrease the contact line velocity once motion is initiated.

**Liquid Transfer Printing Using Patterned Surfaces.** The theory of the dynamics of contact line motion during liquid transfer also explains the differences in volumes of liquid transferred for the three different relief features in Figure 3. In the case of the shallow hole (Figure 3a), the sidewalls of the feature induce a change in the direction in which the three-phase line moves (Schematic, Figure 3a). Since the contact line velocity is a function of the local dynamics at the contact line only,<sup>43</sup> we can safely assume that the magnitude of the velocity remains unchanged. Thus, introducing a shallow holelike feature on the PDMS surface is equivalent to slowing down the three-phase line velocity to  $U \cos \theta$  on the ordinary, flat PDMS surface, where  $U$  is the contact line velocity on the untextured PDMS surface and  $\theta$  is the angle that the walls of the hole make with respect to the horizontal surface. Therefore, the holelike feature increases the amount of liquid transferred to the PDMS surface from the gold substrate, for the same value of gripper velocity. The three-phase line velocity on the post (Schematic, Figure 3b) and the truncated pyramid (Schematic, Figure 3c) surfaces would also be equal to  $U$ , relative to the gripper surface. The velocity relative to a ground frame of reference would be  $U + V$  for the post relief structure and  $U + V \sin \alpha$  for the pyramid structure, where  $V$  is the gripper retraction velocity and  $\alpha$  is the angle the pyramid walls make with the horizontal plane. Thus, the minimum amount of liquid transferred from a gold substrate would be to the post relief structure ( $U + V$ ), followed by the pyramid print-head ( $U$

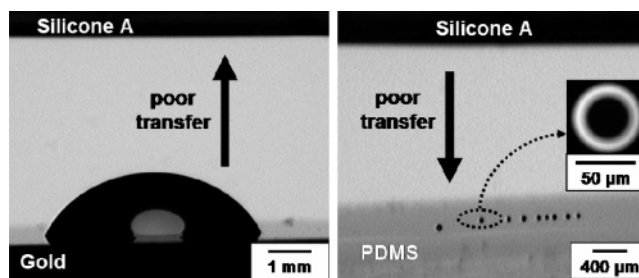


**Figure 6.** Optical micrographs of a two-step transfer printing sequence to create a patterned array of  $50 \mu\text{m}$  droplets (each  $\sim 30$  pL in volume), starting from a 4-mm droplet ( $5 \mu\text{L}$ ). Individual dried out droplets containing fluorescent nanoparticles were visualized with fluorescence microscopy (inset).

+  $V \sin \alpha$ ) for the same value of gripper velocity. The maximum amount of liquid transferred from the gold will be to the surface with the holelike relief since the three-phase line velocity ( $U \cos \theta$ ) is minimal for this surface. Our observations also indicate that the volume of liquid transferred decreases with a reduction in print-head size (parts a and c of Figure 4) and for a pyramidal relief structure with zero tip width no liquid is transferred (not shown). As expected, the percentage of liquid transferred to the relief structures decreases with a decrease in the receding angle of the substrate material (Figure 4) and increases with a decrease in initial volume of liquid on the substrate (parts b and d of Figure 4).

**Double Transfer Printing.** We demonstrate the use of some of these parameters in printing a simple pattern of picoliter-sized droplets on a PDMS surface starting from a much larger droplet, serving as a reservoir (Figure 6). A dilute aqueous solution of fluorescent nanoparticles is used as the liquid. We begin with a large volume of liquid ( $5 \mu\text{L}$ ) and we use a simple two-step procedure that involves the transfer of the liquid from a substrate (gold) to a gripper (silicone A) and then from the silicone A surface, now serving as a substrate to a new gripper (PDMS). In each step, the droplet is compressed and the gripper is retracted at a rate of  $25 \mu\text{m/s}$ . Intentional poor transfer to silicone A from the gold substrate results in the transfer of a 10-nL droplet, which is 500 times smaller than the volume of the initial droplet. In the second step, poor transfer from silicone A to the PDMS gripper results in the transfer of droplets, with a diameter of about  $50 \mu\text{m}$ , which are  $\sim 30$  pL in volume. These droplets are  $6 \times 10^6$  times smaller than the volume of the original droplet ( $5 \mu\text{L}$ ). We used the XY stage on which the substrate is mounted to create a line of such droplets with a minimum spacing of  $100 \mu\text{m}$  (Figure 6). Smaller separation gaps between the location of consecutive liquid transfer steps result in coalescence of neighboring droplets.

**Double Transfer Printing Using Stamps with Relief Features.** The key to minimizing the final droplet size is to reduce the volume of liquid transferred within each step of the procedure. In subsequent experiments we used PDMS relief structures to minimize the volume of liquid picked up in the first transfer step. For all the experiments in Figure 7, the first substrate is gold, from which liquid is transferred onto a PDMS stamp. The surface of the stamp is either flat (Figure 7a), or has patterned relief features like pyramids (Figure 7b) or posts (Figure 7c). This stamp is then used to transfer the small liquid volumes to a flat PDMS surface, which serves as the final gripper surface to which we print. We used 10% glycerol in DI water in these experiments, since the hygroscopic nature of glycerol slows down the evaporation rate of the small liquid droplets, and its low volume percentage does not appreciably alter the transfer characteristics of the liquid when compared to water. As in previous experiments, the gripper retraction velocity in both

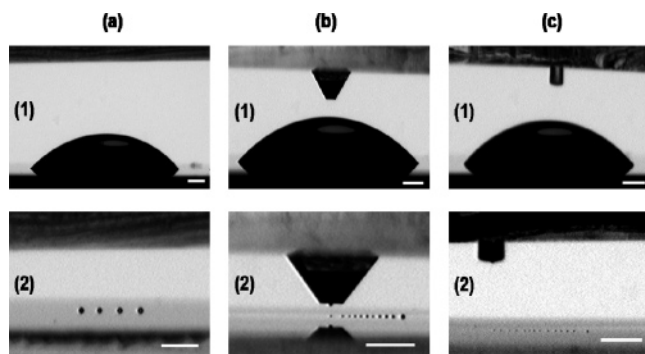


**Figure 7.** Optical micrographs of double transfer experiments using different PDMS stamp surfaces. For all experiments the liquid used is 10% glycerol in deionized water, gold is used as the first substrate, PDMS is used as the final gripper surface, the initial liquid volume is  $5 \mu\text{L}$ , and the gripper retraction rate is  $25 \mu\text{m/s}$ , unless noted otherwise. The images labeled (1) and (2) represent the initial liquid droplet and the final patterned droplets, respectively. Scale bars:  $400 \mu\text{m}$ . (a) Double transfer using an untextured flat PDMS surface as a stamp. The average size of the final patterned droplet is  $100 \pm 5 \mu\text{m}$ . (b) Double transfer using a pyramidal relief structure in PDMS as a stamp. The print-head size is  $200 \mu\text{m}$ , and the average size of final patterned droplet is  $50 \pm 5 \mu\text{m}$ . (c) Double transfer using a  $200 \mu\text{m}$  post relief in PDMS as a stamp. The size of the final patterned droplet is  $30 \pm 5 \mu\text{m}$ .

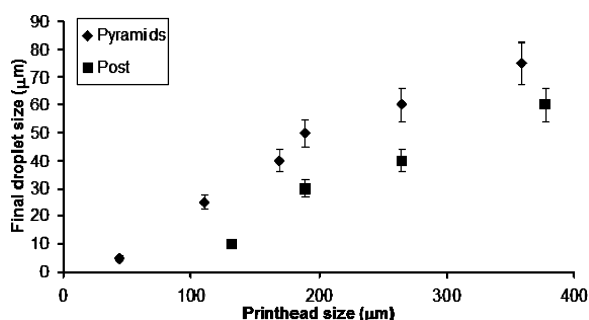


**Figure 8.** Final patterned droplet diameter as a function of print-head size. For all experiments, the liquid is 10% glycerol in deionized water, initial liquid volume is  $5 \mu\text{L}$ , gold is used as the first substrate, PDMS is the final gripper surface to which we print, and gripper retraction rate is  $25 \mu\text{m/s}$ .

transfer steps is  $25 \mu\text{m/s}$  and the initial volume of liquid is  $5 \mu\text{L}$ . The post diameter and the width of the pyramid tip are both  $200 \mu\text{m}$ . As shown in Figure 7, the final patterned droplet diameter is smallest for the post feature.

The graphs shown in Figure 8 compare the average diameter of the final patterned droplets for different print-head sizes. As expected, the droplet diameter decreases with print-head size. Our observations also indicate that scaling down of droplet sizes is easier if we use a post-shaped relief feature on PDMS instead of a pyramid-shaped feature. An increase in the retraction velocity from  $25$  to  $50 \mu\text{m/s}$  increases the diameter of the final patterned droplet by an average of  $10 \mu\text{m}$ . The double transfer technique that we propose here does not require a one-to-one correspondence between the size of the final pattern and the print-head size. Actually, we can print droplets that are significantly smaller in diameter than the width of the tip, for example,  $5 \mu\text{m}$  droplets were printed using pyramids with a  $50 \mu\text{m}$  tip. This eliminates the requirement for lithographically patterned stamps to have features that are of a size equal to or smaller than the features one wishes to print.

In Figure 9, we demonstrate the pick-up and transfer of an array of droplets using the double transfer procedure. The final printed droplets have an average diameter of  $40 \pm 10 \mu\text{m}$ , and

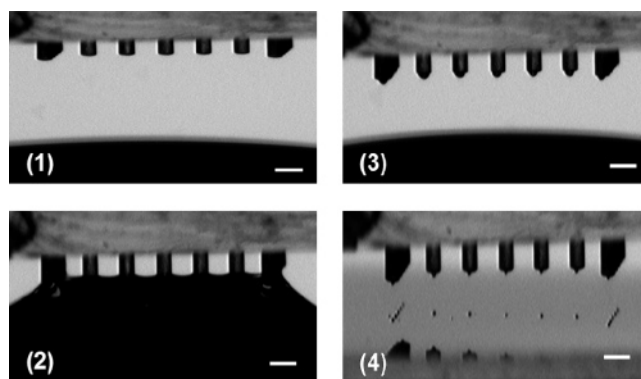


**Figure 9.** Optical micrographs of the sequence of events in the double transfer of a pattern/array of droplets onto a PDMS substrate. The liquid used is 10% glycerol in deionized water, the initial liquid volume is  $50 \mu\text{L}$ , and the gripper retraction velocity is  $25 \mu\text{m/s}$ . Scale bars:  $300 \mu\text{m}$ . The final pattern printed is an “I”, and the average printed droplet size is  $40 \pm 10 \mu\text{m}$ .

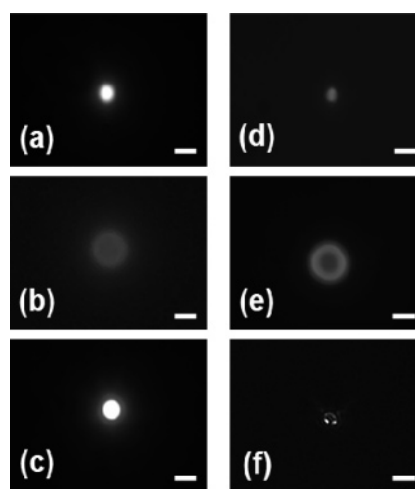


**Figure 10.** Fluorescent images of droplets obtained via double transfer printing onto a PDMS gripper surface using a pyramid relief structure of  $40\text{--}50 \mu\text{m}$ . The initial volume of liquid used is  $10 \mu\text{L}$ , gold is used as the first substrate, and the gripper retraction velocity is  $25 \mu\text{m/s}$ . Scale bars:  $5 \mu\text{m}$ . (a) AlexaFluor 488 hydroxylamine dye, exposure time  $300 \text{ ms}$ . (b) AlexaFluor 647 hydroxylamine dye, exposure time  $850 \text{ ms}$ . (c) Tetramethylrhodamine biocytin, exposure time  $500 \text{ ms}$ . (d) Fluorescent nanoparticles, exposure time  $900 \text{ ms}$ . (e)  $5 \text{ nm}$  colloidal gold conjugate and AlexaFluor 488 labeled streptavidin, exposure time  $1.5 \text{ s}$ . (f) Amino-PEG quantum dots, exposure time  $2.5 \text{ s}$ .

they are printed in the pattern of the letter “I”. Transferring a wide-area pattern of liquid droplets with high fidelity requires that the droplets be centered on the patterned relief structures at the end of the first transfer step. Thus, the print-head surface must be parallel with the surface of the liquid on the first substrate. A minimum pitch length between neighboring relief structures is needed to prevent the transferred droplet from bridging between these two structures. The print-head surface must also be parallel to the target PDMS surface to get a low variance in the size of the patterned droplets.

The images in Figure 10 demonstrate the flexibility of the double transfer procedure in the printing of small volumes of different types of inks onto a PDMS substrate. The droplets were transferred using different pyramidal relief structures that were  $40\text{--}50 \mu\text{m}$  in tip width. The final volume of liquid transferred to the PDMS surface is of the order of  $70 \text{ fL}$ , which is 8 orders of magnitude smaller than the original volume of liquid used ( $10$

$\mu\text{L}$ ). Fluorescence microscopy was used to enable visualization of these small droplets, on the order of  $5\ \mu\text{m}$  each.

### Conclusion

We have identified a set of critical parameters that determine the extent of transfer of liquid from one surface to another in situations where gravity does not play a significant role, and we compared our results with related reports published in literature. On the basis of our experimental observations, we have outlined a two-step mechanism to explain the transfer process, which is in qualitative agreement with all our experimental observations as well as those reported in literature. We also used this model to explain transfer to and from stamps with relief structures and demonstrated the use of some of the identified key parameters to create features with a reproducible lateral size of  $5\ \mu\text{m}$  ( $\sim 70\ \text{fL}$  volume), from an initial drop size of  $5\ \text{mm}$  ( $\sim 10\ \mu\text{L}$  volume), utilizing a two-step liquid transfer procedure. The resulting droplet

of  $70\ \text{fL}$  is  $1.5 \times 10^8$  times smaller than the volume of the initial droplet ( $\sim 10\ \mu\text{L}$ ). Subsequent work will focus on describing the flow field within a liquid bridge, by solving the nondimensional Navier–Stokes equation and the accompanying dimensionless boundary conditions that describe three-phase line motion at each solid surface. The analysis will yield the nondimensional numbers that characterize the liquid transfer process and a maximum value for the gripper retraction velocity that will still permit complete transfer.

**Acknowledgment.** We thank Deepkishore Mukhopadhyay for his help in growing the nitride films. This work was performed within Nano-CEMMS; UIUC's Nano-Science and Engineering Center (NSEC), supported by the National Science Foundation under Award No. DMI-0328162.

LA063266D